Gallium structure on the Si(111)-(7 × 7) surface: influence of Ga coverage and temperature

2007 J. Phys.: Condens. Matter 19 016011

(http://iopscience.iop.org/0953-8984/19/1/016011)

INSTITUTE OF PHYSICS PUBLISHING JOURNAL OF PHYSICS: CONDENSED MATTER

J. Phys.: Condens. Matter **19** (2007) 016011 (15pp) doi:10.1088/0953-8984/19/1/016011

Gallium structure on the Si(111)-(7 × 7) surface: influence of Ga coverage and temperature

J Čechal, M Kolíbal, P Kostelník and T Šikola

Institute of Physical Engineering, Brno University of Technology, Technicka 2896/2, 616 69 Brno, Czech Republic

E-mail: cechal@fme.vutbr.cz

Received 30 August 2006, in final form 24 October 2006
Published 7 December 2006
Online at stacks.iop.org/JPhysCM/19/016011

Abstract

The results of gallium deposition on the Si(111)-(7 × 7) surface at different substrate temperatures (−183, RT, 300, 490 and 530 °C) as well as the influence of subsequent annealing of the prepared layers are presented. The gallium structure was monitored by low-energy electron diffraction (LEED) and synchrotron radiation photoelectron spectroscopy (SR-PES). A detailed analysis of photoelectron spectra was carried out and three different Ga 3d peak components recognized—the first one was related to the $(\sqrt{3} \times \sqrt{3})$ R30° reconstruction, the second to gallium island bases, and the third one to metallic gallium deposited on these bases. Depending on substrate temperature either only the island bases were formed (over 490 °C) or these bases were covered with extra gallium atoms in an additional layer (300 °C). In the case of room (low) temperature deposition only a weak interaction of gallium with the (7 × 7) substrate and a non-ordered growth were found. If the gallium coverage exceeded a critical value the gallium formed small droplets on the silicon surface. Annealing of the deposited layers showed differences between the second and the third gallium layer. In addition to previously reported structures a new $(3\sqrt{3} \times 3\sqrt{3})$ R30° reconstruction was observed after high temperature deposition followed by annealing to 530 °C. This structure was stable in a narrow temperature range and forms an intermediate step between the $(\sqrt{3} \times \sqrt{3})$ R30° reconstruction and the island structure.

(Some figures in this article are in colour only in the electronic version)

1. Introduction

Adsorption of gallium atoms on silicon surfaces has been studied extensively in recent decades for its importance in the heteroepitaxy of III–V semiconductors and a special behaviour given by the distinct nature of atomic bonding in semiconductor substrates and metallic

layers. Various attempts to use these specific heterostructures as a platform for the self-assembled growth of nanostructures have been made and, recently, also to fabricate Ga metallic nanostructures by the selective growth on semiconductor surfaces patterned by nanolithographic methods (e.g. e-beam lithography, SPM local oxidation) [1, 2]. Hence, the understanding of the behaviour of Ga on Si surfaces at different temperatures and a wide range of coverages is a very important issue. Gallium superstructures on the Si(111)-(7 × 7) surface (coverages up to 1 ML) have already been studied mostly by such methods as low energy electron diffraction [3], the x-ray standing-wave technique [4, 5, 7], scanning tunnelling microscopy [5–10], electron energy loss spectroscopy [11], and photoelectron diffraction [12].

It has been observed that the gallium structure on the Si(111)-(7 × 7) surface strongly depends on gallium coverage and deposition and/or annealing temperature. The deposition of a small amount of gallium corresponding to coverages of 0.24–0.28 ML (1 ML is equivalent to 7.83×10^{14} atoms cm^{-2} for the Si(111) unreconstructed surface) at room or enhanced (up to 350 °C) temperature leads to the formation of magic clusters [10, 13, 14]. For a coverage of 1/3 ML of Ga and deposition (annealing, respectively) temperature 550 °C, the $(\sqrt{3} \times \sqrt{3})$ R30° surface reconstruction was found. Gallium atoms (sp^3 hybridization) occupy half of the fourfold coordinated T_4 sites [3, 5, 12] and completely terminate all the silicon surface dangling bonds.

The further increase of Ga coverage up to 1 ML at elevated temperature leads to an incommensurate structure with an approximate periodicity of 2.4 nm formation [4, 6]. Within a coverage range of 0.7–1 ML three different incommensurate structures—(6.3 × 6.3), (11 × 11) and $(6.3\sqrt{3} \times 6.3\sqrt{3})$ R30°—were observed by STM after annealing the Ga layers at 550 °C [9]. In these structures Ga atoms occupy the substitutional positions in the top half of the Si(111) double plane [4, 6], forming a Ga–Si bilayer ($sp^3 \rightarrow sp^2$ re-hybridization of gallium atoms takes place).

Depending on the type of deposition and annealing, new structures and features can be obtained. For instance, based on the STM measurements [8] and theoretical calculations [15] it was found that during the additional deposition of 1/6 Ga ML on the $(\sqrt{3} \times \sqrt{3})$ R30° at elevated temperatures the Ga superstructure triangular clusters (with two to five atoms on their side) and incommensurate islands were formed.

To recognize processes of island formation having a possible application in the nanostructure fabrication, our study deals with a wide range of gallium coverages (up to 5 ML) on Si(111)-(7 × 7) substrates. Hence, synchrotron radiation photoelectron spectroscopy (SR-PES) capable of complex monitoring of gallium surfaces up to a few monolayers was used. As a reference method helping to recognize individual Ga superstructures, LEED was of essential importance.

2. Sample preparation and analysis

The experiments were carried out at the Materials Science Beamline of the Elettra Synchrotron Light Laboratory in Trieste in a UHV chamber with a base pressure of 2×10^{-8} Pa. Two series of experiments were carried out, differing from each other in distinct incoming radiation intensities (as electron beam energy in the synchrotron storage ring was 2.0 and 2.4 GeV, respectively) and in the types of applied gallium effusion cells (home made versus a commercial one). No systematic changes in the results between these two series have been observed.

The Si samples were cut from an n-type (Sb-doped) silicon wafer with a resistivity of 0.006 Ω cm. The samples were flash-annealed at 1250 °C several times for 10–20 s (the pressure being held below 1.5×10^{-7} Pa). After the final flash each sample was slowly cooled down (≈0.5 °C s^{-1}) from a temperature of 850 °C to the deposition temperature in

order to obtain a high quality Si(111)-(7 × 7) surface. The substrate structure and purity was checked by LEED (Specs) and SR-PES measurements, respectively. The samples were heated up resistively by a direct flow of electron current through them and their temperature was measured by a pyrometer and chromel–alumel thermocouple attached to the rear side of the sample holder. The estimated error of the temperature measurement was 20 °C.

Gallium was deposited by a home-made effusion cell at a maximum deposition rate of 0.5 ML h^{-1} in the first series of experiments and by a commercial e-beam effusion cell (Omicron EFM3/4) at a deposition rate of 1.2 ML h^{-1} in the second series. The deposition rate was calibrated according to known surface structures and reconstructions. The pressure during deposition was lower than 7×10^{-8} Pa. In the case of elevated deposition temperatures all the measurements were carried out after the sample was cooled down to room temperature.

The photoelectron spectroscopy analysis was carried out using a hemispherical analyser (Specs Phoibos 150). The spectrometer was operated in the fixed-analyser-transmission mode with pass energy of 2 eV. The spectra were acquired in 0.1 eV steps and the beamline and monochromator slits were set to get a resolving power of 2000 (the total instrumental energy resolution was better than 0.1 eV). The diameter of an analysed area was smaller than 100 μm.

All the measured spectra were normalized to the incident radiation intensity, which was falling over time due to a continuous decrease of electron current in the storage ring. This intensity was monitored by the current induced in a metal mesh placed across the radiation beam in front of the UHV chamber. The incident radiation energy was calibrated by measuring the Fermi edge of the clean Si(111)-(7 × 7) surface. The photon energy was (144.29 ± 0.03) eV during the first series of experiments and (144.35 ± 0.03) eV during the second series, respectively. The majority of spectra were taken at the normal emission geometry—detected photoelectrons were leaving the surface under the normal direction and the incidence angle of exciting radiation was 60° with respect to the surface normal. If not specified otherwise, all the spectra, graphs, and tables are related to this mode. Alternatively, other emission angles were used, but the angle between the emitted photoelectrons and the incident photon beam remained the same (60°).

An additional analysis was carried out at the authors' home institution. The EFM3/4 effusion cell was used in a UHV chamber with a base pressure of 1×10^{-7} Pa and the LEED analysis was done by the ErLEED instrument (Specs).

3. Results and discussion

Consecutive Ga depositions at five different temperatures in two series of experiments were carried out. The first series included a room temperature deposition (RT), low temperature deposition at −183 °C (LT) (the sample cooled down indirectly by liquid nitrogen), and, finally, an enhanced temperature deposition at 300 °C (ET). The gallium layers prepared at room and enhanced temperatures were then incrementally annealed at higher and higher temperatures. In the second series high temperature depositions (HT) at temperatures of 490 and 530 °C followed by annealing, and additional RT deposition and annealing to confirm the results of the first series, were performed. After each deposition or annealing the photoelectron spectra and LEED patterns were taken. These measurements were made at sample low or room temperature (after the sample cooled down to RT in the case of elevated temperature deposition or annealing).

3.1. Spectroscopic measurements

The Si 2p spectrum taken from a clean Si(111) sample with the (7 × 7) surface reconstruction and its deconvolution into components is shown in figure 1(a). The peak decomposition was

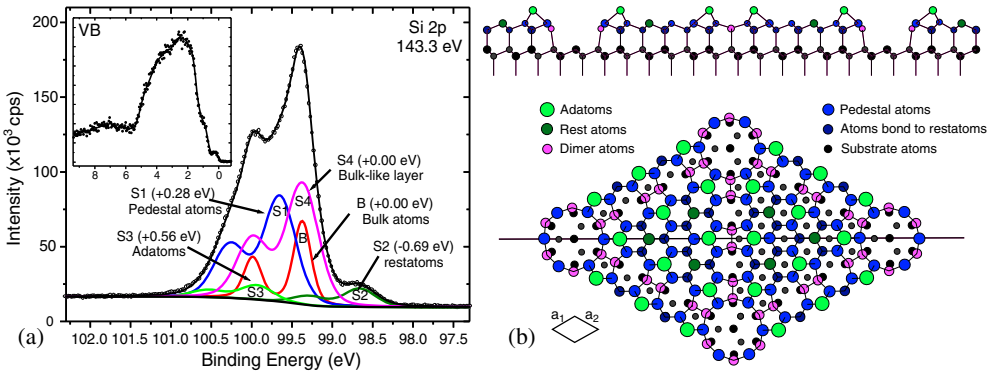

Figure 1. (a) The Si 2p spectrum of Si(111)-(7 × 7) and (b) a schematic representation of this reconstruction. The inset in (a) shows the valence band spectra of Si(111)-(7 × 7).

Table 1. The surface-core level shifts (SCLSs), Gaussian widths (GWs) and assignment of Si $2p^{3/2}$ peak components. The spin–orbit splitting 0.615 eV, branching ratio 0.5 and Lorentzian width 0.085 eV were common for all the components.

Component	SCLS (eV)	GW (eV)	Peak assignment
Bulk (B)	0.00	0.21	Bulk silicon
S1	+0.28	0.42	36 pedestal atoms and 18 atoms bound to restatoms
S2	−0.71	0.42	6 restatoms
S3	+0.56	0.42	12 adatoms
S4	0.00	0.42	18 dimer atoms, 12 atoms immediately under the adatoms and 98 atoms underneath (bulk-like layer)
Si-Ga1	−0.22	0.32	Ga in $(\sqrt{3} \times \sqrt{3})$ R30°
Si-Ga2	−0.25	0.42	Ga island

carried out using Voigt functions according to the paper of Paggel *et al* [16]. The spin–orbit splitting 0.615 eV, branching ratio 0.5, and Lorentzian width 0.085 eV were common for of all the peaks. The peak positions, Gaussian widths, and peak assignment according to [16, 17] are summarized in table 1.

The bulk peak position (Si $2p^{3/2}$ − B) related to the Fermi level was (99.38 ± 0.02) eV. With the reported energy difference between the Si 2p line and the valence band maximum (E_B(Si $2p^{3/2}$ − B) − E_{VBM} = 98.74 eV) [18] this corresponds to the surface Fermi level position $E_F - E_{VBM}$ = 0.64 eV, which agrees well with the previously reported value (0.63 ± 0.05) eV [18]. After cooling down the substrate to a temperature of −183 °C the shift of the whole spectrum by 0.12 eV towards a higher binding energy was observed. This shift was most probably caused by a surface photovoltaic effect [19]. A similar effect was observed by Landemark *et al* [20] after cooling down the Si(100) sample as well.

During gallium deposition the progressive shift of all the spectra towards the lower binding energies due to change of band bending was observed. The maximum shift after deposition of 5 ML of Ga was (0.32 ± 0.03) eV. This shift corresponds to the surface Fermi level position $E_F - E_{VBM}$ = 0.32 eV, which agrees well with a value of 0.35 eV reported by Althainz *et al* [21] for the Ga/p–Si(111) interface. Additionally, the difference in the work function between the bare Si(111)-(7 × 7) surface and the same surface covered with 1.6 ML of Ga was measured as well. The obtained value, (0.23 ± 0.05) eV, is in agreement with the previously reported one [22].

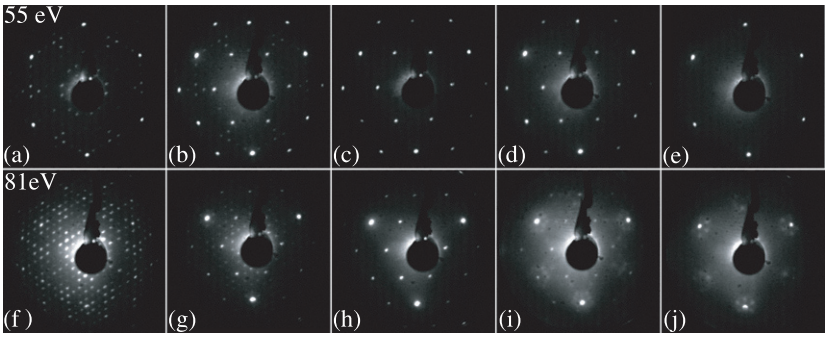

Figure 2. LEED patterns for two electron energies—55 eV (top row) and 81 eV (bottom row)—and for different gallium coverages during HT deposition (530 °C). (a), (f) Si(111) 7 × 7; (c), (h) 0.3 ML − $(\sqrt{3} \times \sqrt{3})$ R30°; (e), (j) 0.9 ML − $(6.3\sqrt{3} \times 6.3\sqrt{3})$ R30°. Interlaying figures (b), (g) and (d), (i) show a mixture of phases from the neighbouring figures at coverages of 0.2 and 0.6 ML, respectively.

In the valence band spectrum of Si(111)-(7 × 7) (see inset in figure 1) a sharp Fermi edge is visible due to a quasimetallic character of this surface [23]. Additionally, the contributions of surface state bands S1 and S2 at 0.35 and 0.8 eV related to adatoms and restatoms, respectively [24], can be recognized here as well.

The following presentation of the achieved results will be commenced with the experiments carried out at higher deposition temperatures as their results lead to better understanding of the behaviour of Ga layers prepared at lower temperatures.

3.2. High temperature deposition

The high temperature depositions were carried out at the temperatures of 490 °C (HT-1) and 530 °C (HT-2). Typical LEED patterns taken during the HT-2 deposition are shown in figure 2. The final structure (figures 2(e), (j)) most probably corresponds to the $(6.3\sqrt{3} \times 6.3\sqrt{3})$ R30° rather than (6.3 × 6.3) surface reconstruction [25]. In the text below the term 'island reconstruction' will be used to denote this surface structure, since both mentioned reconstructions are similar and are associated with gallium islands.

The observed LEED patterns progressively change with the gallium coverage. In the case of HT-1 (490 °C) deposition the (7 × 7) substrate pattern was still observed after the Ga deposition of 0.1 ML. For the sample with 0.2 ML Ga coverage the mixture of the (7 × 7) and $(\sqrt{3} \times \sqrt{3})$ R30° surface reconstruction was observed. The $(\sqrt{3} \times \sqrt{3})$ R30° reconstruction is the only structure observed for Ga coverages of 0.3–0.4 ML. From 0.4 ML up to 0.5 ML a mixture of the $(\sqrt{3} \times \sqrt{3})$ R30° and island reconstructions was observed. For Ga coverages above 0.6 ML the $(\sqrt{3} \times \sqrt{3})$ R30° reconstruction disappeared and only the island reconstruction was observed.

The LEED pattern changes are gentler in the case of HT-2 (530 °C) deposition. The $(\sqrt{3} \times \sqrt{3})$ R30° reconstruction was observed as the only one within the range 0.3–0.5 ML and up to 0.8 ML a mixture of the $(\sqrt{3} \times \sqrt{3})$ R30° and the island reconstruction was observed. The island reconstruction remained the only one above a coverage of 0.9 ML. The evolution of diffraction patterns is consistent with the previous LEED studies [3, 22, 25].

Concerning spectra taken by SR-PES there was an increase of the Ga 3d peak intensity and a simultaneous decrease of the Si 2p peak intensity with increasing gallium coverage. The fitting of the Ga 3d peak for different gallium coverages of the HT-2 (530 °C) sample is presented in figure 3. It was possible to fit the Ga 3d peak by just two components. The first

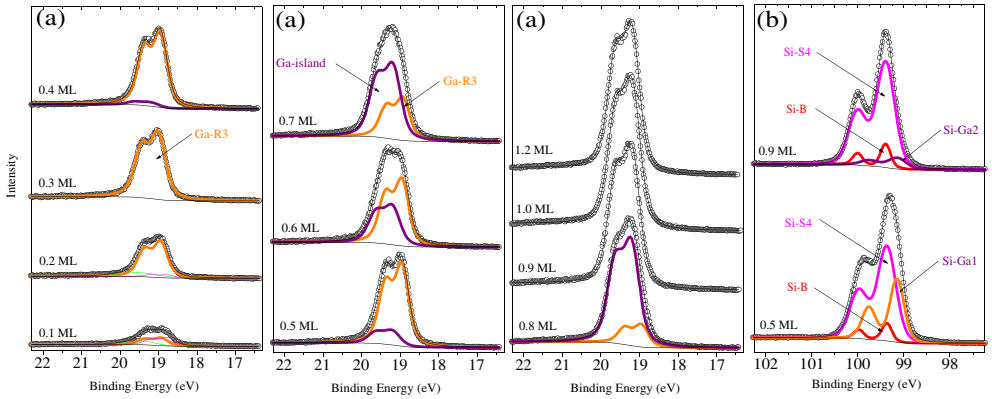

Figure 3. (a) Ga 3d peak during HT-2 (530 °C) deposition. There are two basic peaks related to $(\sqrt{3} \times \sqrt{3})$ R30° (Ga-R3) and island (Ga-island) reconstructions. (b) Si 2p peak fit for $(\sqrt{3} \times \sqrt{3})$ R30° and island reconstructions. The peaks were corrected for band bending shift according to the Si 2p bulk peak position.

Table 2. The relative peak shifts (RPSs), Gaussian widths (GWs), branching ratios, asymmetry parameters and peak assignments of Ga $3d^{5/2}$ peak components. The spin–orbit splitting 0.43 eV and Lorentzian width 0.21 eV was common for all components.

Component	RPS (eV)	GW (eV)	Branching ratio	Asymmetry	Peak assignment
Ga-$\sqrt{3}$ (Ga-R3)	0.00	0.30	0.77	—	$(\sqrt{3} \times \sqrt{3})$ R30°
Ga-island	+0.25	0.35–0.37	0.80	—	Ga island bases
Ga-island	0.00	0.35–0.45	0.80	—	Ga island bases
Ga-metallic	−0.37	0.20	0.75	0.15	Metallic gallium

one is related to the gallium atoms forming the $(\sqrt{3} \times \sqrt{3})$ R30° reconstruction and the second one to the island reconstruction. The intensity development of these two peaks is in a good agreement with the observed diffraction patterns. When the sharp diffraction pattern showed the presence of the $(\sqrt{3} \times \sqrt{3})$ R30° reconstruction as the only reconstruction on the surface, the Ga 3d spectrum could be fitted just by one peak (Ga-$\sqrt{3}$). The second peak (Ga-island) started to grow during a further gallium deposition when the Ga coverage exceeded 1/3 ML. At the end of the deposition when the Ga 3d peak intensity saturates, the spectrum can be fitted using this second peak only. The saturated intensity of the Ga 3d peak and the presence of a sharp diffraction pattern of island reconstruction leads to the conclusion that the surface is covered by 2D Ga islands which are bases of further 3D Ga island growth. To fit the Ga 3d peak corresponding to the early stages of the deposition two additional peaks (not shown here) were necessary for keeping both the Ga-$\sqrt{3}$ peak position and other parameters. These two peaks are probably related to two different states of gallium atoms forming the magic clusters (the side and corner atoms). The Ga 3d peak was fitted using Voigt functions. The spin–orbit splitting 0.43 eV and Lorentzian width 0.21 eV were common values for all the Ga 3d peaks. The peak positions, Gaussian widths, branching ratios and peaks assignment are summarized in table 2. The difference in branching ratios is possibly caused by a photoelectron diffraction effect [26].

The spectrum of bare silicon with the (7 × 7) reconstruction was described in section 3.1. The same fitting procedure of the Si 2p peak as was used for the bare surface can be applied to the spectra, but there was a need for one more peak related to the silicon atoms bound to

gallium. The intensity of the peak related to the restatoms (Si-S2) halves after the deposition of 0.1 ML of Ga; with further deposition its intensity decreases and the peak disappears when a Ga coverage of 0.5 ML is achieved. The surface-core level shifts (SCLS) of the restatom peak slightly changed to −0.75 eV after the deposition of 0.1 ML of Ga. The intensity of the peak related to the adatoms (Si-S3) decreased in the same way as intensity of the restatom peak, but it disappeared already at a Ga coverage of 0.3 ML. A similar evolution of the intensity as for the Si-S2 peak was observed for the Si-S1 peak. From a coverage of 0.5 ML up the Si 2p peak can be fitted only by three peaks—the bulk (Si-B), the bulk-like (Si-S4) and a new peak marked as Si-Ga1 with SCLS of −0.22 eV (see figure 3(b)). The new peak is probably related to the silicon atoms bound to gallium atoms forming the $(\sqrt{3} \times \sqrt{3})$ R30° reconstruction in the T_4 site. A similar shape of the Si 2p spectrum was observed during an indium deposition [27] on the Si(111)-(7 × 7) surface as well—the Si 2p peak consisted of the main bulk component and an additional component shifted by 0.28 eV to lower binding energies and assigned to Si atoms bound to In atoms sitting in the T_4 site. The shift of the Si-Ga1 component to a lower binding energy suggests a charge transfer from the gallium atom to the silicon atoms in the $(\sqrt{3} \times \sqrt{3})$ R30° structure. The lower value of SCLS of the Si-Ga1 peak compared to the Si–In peak shift results from the lower charge transfer. This is consistent with a lower electronegativity difference between Ga and Si atoms than between In and Si atoms. With a growing coverage the intensity of the Si-Ga1 peak decreases and finally a new peak component with SCLS of −0.25 eV appears (see figure 3(b)). This new peak (Si-Ga2) can be assigned to silicon atoms forming a Ga–Si bilayer in Ga islands according to the model suggested in [8]. The parameters of peaks related to Si–Ga bonds are summarized in table 1.

There were characteristic changes in the valence band spectra during the high temperature deposition (both HT-1 and HT-2). A significant decrease of intensity in the near Fermi edge region was observed—the Fermi edge almost disappeared already after the deposition of 0.1 ML of gallium and the restatom step vanished completely. During the formation of the $(\sqrt{3}\times\sqrt{3})$ R30° reconstruction (0.1–0.3 ML for HT-1 and 0.1–0.5 ML for HT-2 coverage) there was a slight increase of intensity in the 0.3–0.5 eV energy region and a noticeable increase in the energy range 1.2–1.4 eV. This agrees well with the ARUPS measurements of $(\sqrt{3} \times \sqrt{3})$ R30° reconstructed surfaces of the group III metals, where surface metal bands were observed at about 0.4 eV and 1.4 eV [28]. During further deposition—an island structure formation at 0.4–0.9 ML and 0.6–1.1 ML coverages for the HT-1 and HT-2 sample, respectively—the intensity in the energy region 0.3–0.5 eV decreased to zero and a significant increase in the 1.7–2.3 eV energy range and a slight decrease in the 3.1–4.8 eV region were observed. No Fermi edge related to metallic gallium was observed when the islands were formed.

The evolution of Ga 3d peak intensity during the HT-1 and HT-2 depositions is plotted in figure 4(a). The intensity linearly increases until the 1/3 ML coverage is obtained and then a sharp (a slight) slope break in the HT-2 (HT-1, respectively) intensity curve occurs. The intensity saturation appears above 0.7 ML (HT-1) and 0.9 ML (HT-2) coverage. The saturated intensity of the Ga 3d peak is a bit lower in the case of HT-2 deposition.

Subsequent annealing of the samples at the same temperatures as deposition ones for 30 min led to a substantial decrease of the Ga 3d peak intensity in the case of the HT-2 sample, but only to its slight decrease for the HT-1 sample (figure 4(a), right). As for the HT-2 sample the intensity decreased to the value corresponding to a coverage close to 1/3 ML, which means that the HT-2 deposition for coverages above 1/3 ML proceeds under dynamic equilibrium between the fluxes of incoming and evaporating loosely bound atoms. Under these conditions a new surface reconstruction was observed (see section 3.3). After the second annealing of this sample at 570 °C gallium was evaporated out from the sample and the Si(111)-(7 × 7) reconstruction appeared again, which was proved by LEED and SR-PES as well.

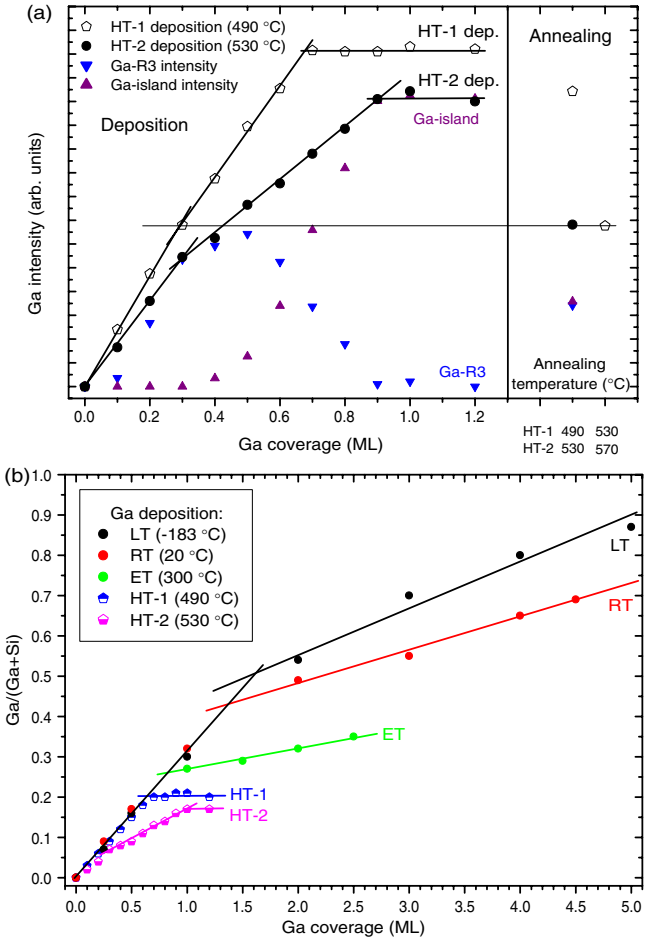

Figure 4. (a) Ga 3d peak intensity during HT-1 (490 °C) and HT-2 (530 °C) depositions and subsequent annealing. The intensities of peaks related to $(\sqrt{3} \times \sqrt{3})$ R30° (Ga-R3) and island (Ga-island) reconstructions for HT-2 deposition. (b) Normalized intensities of the Ga 3d peak for all depositions: LT (−183 °C), RT (20 °C), ET (300 °C), HT-1 (490 °C), and HT-2 (530 °C).

Concerning the HT-1 (490 °C) sample, its annealing at the same temperature as the deposition one leads to the Ga 3d peak intensity corresponding to the saturated intensity for the HT-2 (530 °C) sample. This suggests just a small over-saturation of the surface during deposition being caused by a small amount of weakly bound Ga atoms. After the second annealing (530 °C) the intensity of the Ga 3d peak decreased to the same value as observed after the first annealing of the HT-2 sample, and the same LEED pattern corresponding to a new superstructure appeared.

3.3. The $(3\sqrt{3} \times 3\sqrt{3})$ *R30° surface reconstruction*

The typical LEED patterns taken after annealing the HT-1 or HT-2 sample at 530 °C (see above) are shown in figures 5(a) and (b). This pattern—$(3\sqrt{3} \times 3\sqrt{3})$ R30°—does not correspond to any surface structure reported so far on Ga/Si(111) surfaces. From the Ga 3d peak intensity corresponding to this structure it is apparent that Ga coverage has to be similar to 1/3 ML.

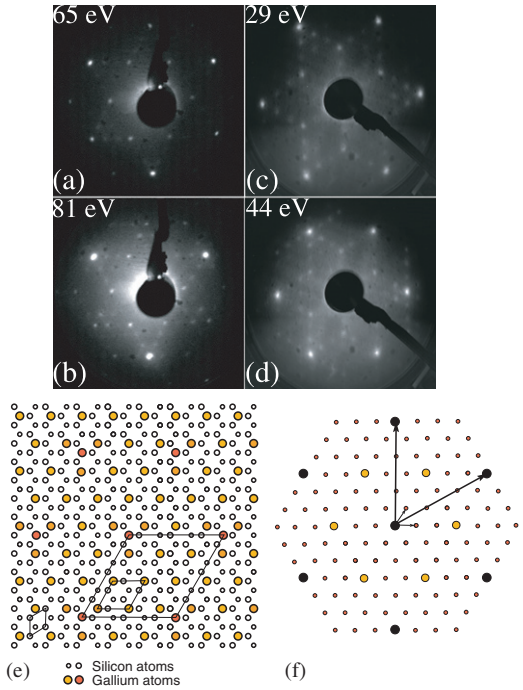

Figure 5. (a)–(d) LEED patterns, (e) schematic model and (f) reciprocal lattice for $(3\sqrt{3} \times 3\sqrt{3})$ R30° reconstruction. The (a) and (b) patterns were taken during the main experiment while the (c) and (d) patterns were recorded during additional experiments at the home laboratory.

Further, it was found that the annealing of the sample with this structure at even higher temperature (550 °C) leads to the $(\sqrt{3} \times \sqrt{3})$ R30° reconstruction formation, indicating that the Ga coverage is a bit higher than 1/3 ML. The model of this structure corresponding to the $(3\sqrt{3}\times3\sqrt{3})$ R30° reconstruction and the related reciprocal lattice are shown in figures 5(e) and (f). The configuration of the reciprocal lattice is in a good agreement with the diffraction pattern of this structure (figures 5(a)–(d)). The gallium coverage derived from this model (0.37 ML) is also proportional to the measured intensity.

In addition to the model presented in figure 5(e) other models of the $(3\sqrt{3} \times 3\sqrt{3})$ R30° structure have been tested as well. In these alternative models the Ga–Si clusters with two to four Ga atoms on their sides were used. These clusters were previously observed after an additional deposition of 1/6 ML of Ga on the Si(111)-$(\sqrt{3} \times \sqrt{3})$ R30°-Ga surface [8]. None of these clusters fits into the $(3\sqrt{3} \times 3\sqrt{3})$ R30° surface reconstruction without significant change of position of the atoms forming the $(\sqrt{3} \times \sqrt{3})$ R30°-Ga reconstruction. Moreover, a large number of silicon dangling bonds remain unsaturated, the theoretical Ga coverage is too high, and/or the observed spectra do not fit to those expected from the supposed model. Hence, the model presented in figure 5(e) might be assigned to the observed $(3\sqrt{3} \times 3\sqrt{3})$ R30° reconstruction. However, to prove this hypothesis LEED I–V curve analysis or STM experiments are necessary.

The theoretical ratio between the number of atoms creating the islands and those of the $(\sqrt{3}\times\sqrt{3})$ R30° reconstruction given by the suggested model is 4:6. One would expect that the intensity ratio of the relevant Ga 3d peak components should correspond to this ratio. However, the experiments revealed variations in the peak shape with emission angle changes and thus in

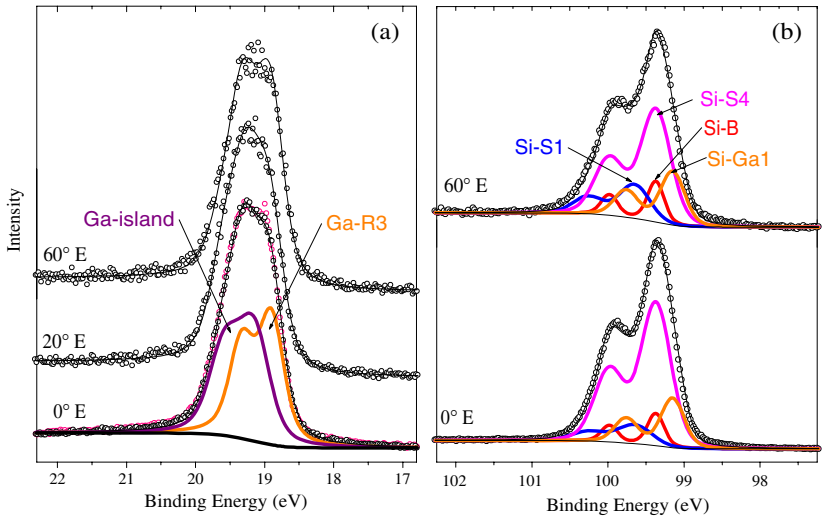

Figure 6. (a) Ga 3d and (b) Si 2p peaks taken from the sample with $(3\sqrt{3} \times 3\sqrt{3})$ R30° reconstruction.

intensity ratios as well. The spectra of the Ga 3d peak related to this superstructure taken at three different emission angles (0°, 20°, and 60°) are shown in figure 6(a). To fit the Ga 3d peak the same two peak components as for the only deposited Ga layers could be used. The intensities of both components were practically the same (50:50) for the normal emission (0°) geometry. When the 20° emission geometry was used, the intensity ratio between the peak related to the islands and the peak corresponding to the $(\sqrt{3} \times \sqrt{3})$ R30° reconstruction was 55:45. Only for the last geometry (60° emission) was the situation as expected—the intensity ratio was 4:6 in favour of the Ga-$\sqrt{3}$ peak. These variations could arise from a photoelectron diffraction effect; however, no calculations have been done so far.

The spectra of the Si 2p peak taken at the 0° and 60° emission geometries (figure 6(b)) are very similar. The peak related to the silicon atom bound to Ga atoms forming the $(\sqrt{3}\times\sqrt{3})$ R30° reconstruction can be identified in the spectrum. Additionally, it was necessary to use the Si-S1 component for fitting the spectrum. The presence of a similar component was observed previously during the In-(2×2) phase formation and it was interpreted as the bulk component shifted due to the different local band bending of two distinct structures coexisting on the surface [27]. The absence of the second component (Si-Ga2) related to the silicon atoms forming the Ga–Si bilayer of the islands supports the presented model. A closer look at the diffraction pattern taken during the deposition at 530 °C (figure 2(i)) reveals a mixture of the $(3\sqrt{3} \times 3\sqrt{3})$ R30° and island reconstructions, indicating that the $(3\sqrt{3} \times 3\sqrt{3})$ R30° structure is a stable intermediate step between $(\sqrt{3} \times \sqrt{3})$ R30° and island reconstruction.

This structure was also observed during additional experiments in our home laboratory after high temperature gallium deposition and subsequent annealing. After 1 ML Ga deposition at a substrate temperature of 430 °C the diffraction pattern corresponding to $(6.3\sqrt{3} \times 6.3\sqrt{3})$ R30° surface reconstruction was observed. Thereafter, the sample was incrementally annealed (each annealing lasted 15 min), and after annealing at 500–530 °C the $(3\sqrt{3} \times 3\sqrt{3})$ R30° reconstruction appeared. The sharpest, best quality pattern was obtained after 520 °C annealing. The corresponding LEED patterns are shown in figures 5(c) and (d). Additional annealing at 540 °C resulted in formation of the $(\sqrt{3} \times \sqrt{3})$ R30° surface reconstruction.

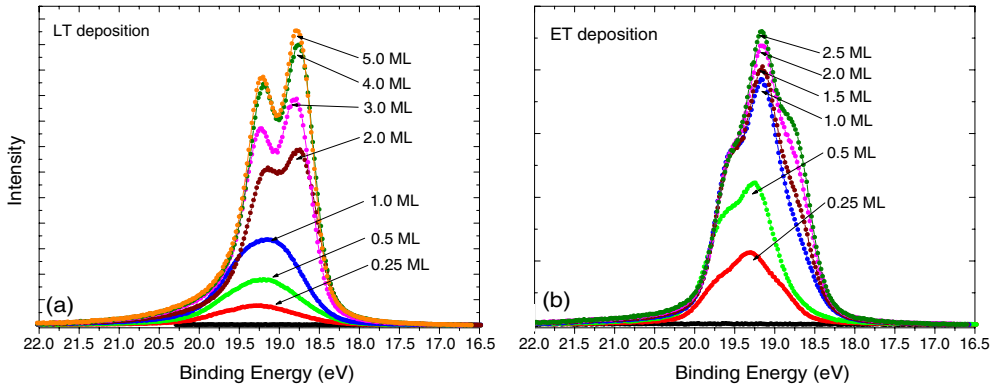

Figure 7. The evolution of Ga 3d peaks during (a) low (−183 °C) and (b) enhanced temperature (300 °C) deposition. The peaks were shifted according to the Si 2p bulk peak position to correct a band bending shift.

3.4. Room and low temperature depositions

Ga depositions were also carried out at room temperature (RT) and low temperature equal to −183 °C (LT). The Si(111)-(7 × 7) diffraction patterns were still observable for 0.25 ML and 0.5 ML Ga coverages, respectively, although the diffraction spots were very weak. After deposition of 1.0 ML the diffraction spots practically disappeared for both temperatures.

The normalized intensities of Ga peaks for all the depositions are shown in figure 4(b). The growth of the unresolved broad Ga 3d peak (figure 7(a)) and a linear increase of its intensity were observed until a slope break occurred (coverages 1.4 ML for RT and 1.6 ML for LT). Then the peak shape changed significantly to a broad doublet peak with a strong asymmetric character. The doublet component splitting in the range of 0.36–0.43 eV suggests that the Ga 3d peak contains more than one component. Based on an annealing experiment (see below) it was possible to decompose the Ga 3d peak into a main asymmetric component related to the metallic gallium and another component (components) assigned to the bases of 3D islands.

The Si spectrum of the RT and LT samples revealed similar behaviour with the growing Ga coverage. The intensity of the Si 2p peak linearly decreases and there is a slope break at the same coverages as observed for gallium. After Ga deposition of 0.25 ML the adatom and restatom peaks nearly disappeared from the silicon spectrum. From 1 ML coverage up only three significant peak components could be found in the spectra—the bulk (Si-B), bulk-like (Si-S4), and the weak Si-Ga2. The overall peak shape was similar to that observed after the island bases were formed at the end of HT deposition and did not change with further deposition.

After the first depositions (0.5 ML) the restatom and adatom contributions, as well as the Fermi edge, disappeared from the valence band spectra. The overall intensity in the valence band region 0–6 eV was decreasing with a further deposition. Finally, the sharp Fermi edge re-appeared after the total deposition of 3 ML, although a weak Fermi edge was observed already at 2 ML coverage (coinciding with the change of the Ga 3d peak shape).

Based on these observations one may conclude that in the case of room and low temperature depositions there is a non-ordered Ga growth and only a weak interaction of deposited gallium with the substrate since the diffraction pattern of the Si(111)-(7 × 7) surface reconstruction was observed up to relatively high coverages (0.5–1 ML). On the other hand, the restatom and adatom Si 2p peaks disappeared from the SR-PES spectra after 0.25 ML Ga

deposition, probably due to forming various bonds between silicon and gallium atoms. If the gallium coverage exceeds a critical amount the gallium layer gains a metallic character (the Fermi edge re-appears) and Ga atoms form droplets on the surface. These droplets on the Si(111)-(7 × 7) surface were observed by AFM and reported in [29].

3.5. Enhanced temperature deposition

This type of deposition was carried out at sample temperature of 300 °C (ET). The Si(111)-(7 × 7) diffraction pattern was still observable after the deposition of 0.25 ML, but contrary to RT and LT depositions it disappeared already after the deposition of 0.5 ML and only a weak substrate (1 × 1) pattern was observed for further depositions.

The shape of the Ga 3d peak after the deposition of 0.25 ML of Ga was similar to what we observed when a mixture of the ($\sqrt{3} \times \sqrt{3}$) R30° and island reconstructions was present on the surface during the HT deposition. For a Ga coverage of 0.5 ML the Ga 3d peak shape corresponded to the island structure. After deposition of 1 ML a new component appeared on the low energy side of the Ga 3d peak and its intensity gradually increased with gallium coverage. A similar component was previously observed by Fritsche *et al* [22], but its origin was not explained. We suggest that this peak is related to metallic gallium forming 3D islands (second gallium layer). However, in this case there are not enough gallium atoms (low coverage) to form a sharp Fermi edge.

The gallium intensity grows linearly up to 0.8 ML coverage when a slope break occurs, resulting in a slower intensity growth afterwards (figure 4). This slope break occurs at the coverage at which the island bases are completely formed; the additional gallium atoms are deposited only on their tops. The evolution of the Si 2p peak is similar to the one previously observed during the LT and RT depositions. After the deposition of 0.25 ML the intensity of restatom and adatom peaks significantly decreases and become zero with a further deposition. For a coverage of 0.5 ML the Si 2p peak shape was similar to the one observed for similar coverages during the HT deposition. Above 1 ML coverage its shape was similar to that observed during the RT deposition and changed only a little with further deposition.

To conclude, the enhanced temperature (300 °C) gallium growth proceeds as an intermediate step between the room and high temperature depositions. The sub-monolayer growth is similar to that at high temperature, but it is much less ordered because diffraction patterns related to the ($\sqrt{3} \times \sqrt{3}$) R30° or island reconstructions were not observed. On the other hand, the gallium and silicon spectra show similarities to the peaks found for these reconstructions. When the island bases are formed the extra gallium atoms sit on their tops.

3.6. Annealing of Ga layers

The layers prepared at room and enhanced temperatures were incrementally annealed to higher and higher temperature (each annealing lasted 15 s) after the final deposition. Concerning the annealing of layers prepared at room temperature the LEED patterns showed no reconstruction pattern during the annealing up to 360 °C. In the temperature range 360–530 °C a weak diffraction pattern of (6.3 × 6.3) structure was observed. The sharpest pattern related to this island structure was observed at a temperature of 530 °C. The further annealing led to a rapid gallium desorption leaving the bare (7 × 7) surface.

The dependence of the normalized Ga 3d peak intensity for samples of different deposition histories on annealing temperature is shown in figure 8(a). In the case of the Ga layer deposited at room temperature (RT) the gallium peak intensity starts to decrease already after the annealing at 70 °C and this decrease continues until the temperature of 360 °C is reached.

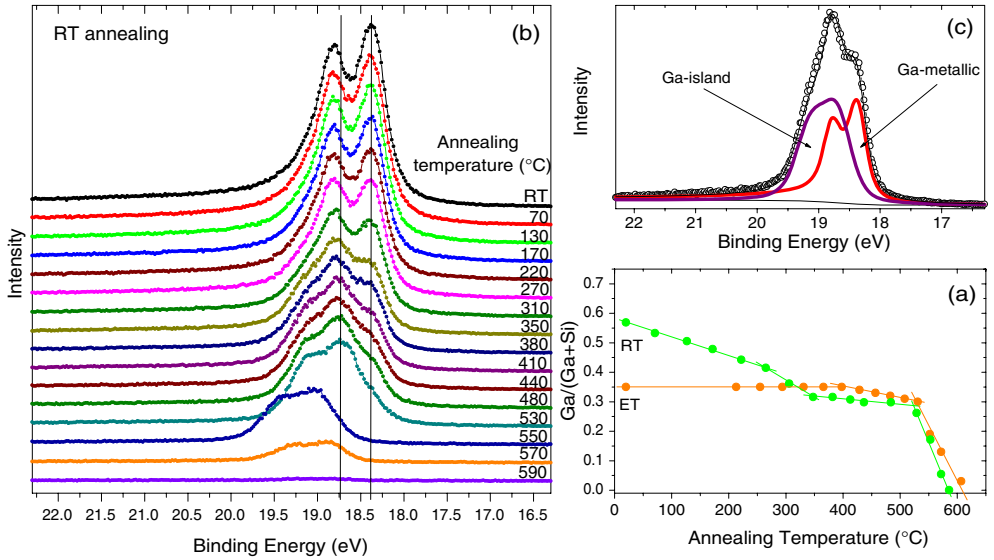

Figure 8. (a) Dependence of normalized peak intensity on annealing temperature for the Ga samples grown at room (RT) and enhanced (ET, 300 °C) temperatures. (b) The evolution of the Ga 3d peak during annealing of the Ga layer deposited at room temperature. (c) Peak fitting in the temperature range 350–550 °C.

On further annealing the gallium peak intensity decreases very slowly up to 530 °C when this behaviour turns to a rapid intensity fall with higher temperatures. The evolution of the Ga 3d-peak shape during annealing the RT sample is shown in figure 8(b). After Ga deposition the Ga 3d peak is formed by one significant component with an asymmetric shape (metallic Ga). As annealing at higher and higher temperatures continues, a second component appears in the spectrum. Hence, in the temperature range 360–530 °C the Ga 3d peak can be fitted by two components (figure 8(c))—one is related to the island bases and another one (shifted by 0.37 eV towards lower binding energies) is linked with the above mentioned metallic gallium. The latter component exhibits a strong asymmetry and it was fitted using the convolution of the Doniach–Sunjic line shape (asymmetry parameter of 0.15) and the Gauss function. A similar peak was also observed during deposition of In for coverages over 0.8 ML [27]. The intensity of the latter peak component continuously decreases with increasing temperature, and after the annealing at 550 °C the Ga 3d peak is formed only by the former component. During this decrease associated with desorption of metallic gallium the Ga-island peak slightly increases due to a lower photoelectron absorption. It was impossible to use this two-peak fitting procedure at annealing temperatures below 360 °C, probably because of a too thick metallic-Ga 'capping' layer exceeding 1 ML and/or due to not well developed island bases. Although the metallic-Ga peak was observed up to the annealing temperature 530 °C, the Fermi edge related to the metallic gallium had already disappeared from the valence band spectra after the annealing at 260 °C. There were also only small changes in the Si 2p peak shape (Ga–Si bilayer). Its intensity slightly increases as the gallium intensity decreases. After all the gallium was desorbed from the surface the Si 2p spectrum related to a Si(111)-(7 × 7) surface reconstruction re-appeared.

In the case of Ga deposition at an enhanced temperature the intensity and the shape of all peaks practically do not change up to a temperature of 400 °C. As shown in figure 8(a), the intensity of the gallium peak slowly decreases within the temperature range 400–530 °C as a

result of desorption of atoms of metallic gallium. Only the Ga-island peak component was observed after annealing at 530 °C. Annealing at higher temperatures led to the fast desorption of all gallium atoms from the sample.

Based on these observations, one can conclude that annealing up to 360–400 °C leads to desorption of metallic gallium (forming 3D islands), leaving the island bases with only one atomic layer on their tops. These gallium atoms slowly desorb in the temperature range 360–530 °C. Annealing at higher temperatures leads to a rapid gallium desorption.

4. Conclusions

The structure of gallium on the Si(111)-(7 × 7) surface was studied by synchrotron radiation photoelectron spectroscopy and low-energy electron diffraction. The deposition of 1/3 ML of Ga at high temperatures (450–550 °C) leads to the well known ($\sqrt{3} \times \sqrt{3}$) R30° structure, which is characterized by the presence of a single peak in the Ga 3d spectrum and three major components in the Si 2p spectrum—bulk and bulk-like ones and a second peak related to Si bonds to Ga.

With further deposition the gallium islands are growing. In the case of high temperature deposition (490 °C) only the island bases (2D islands) are formed, which are accompanied by the appearance of a new peak both in the Ga 3d and Si 2p spectra. If a lower deposition temperature (300 °C) is used, the extra gallium (second layer) is deposited on the previously created island bases forming 3D islands (a new asymmetric component appears in the Ga 3d spectra). The gallium in the second layer has a metallic character.

During the room and low (−183 °C) temperature depositions the non-ordered gallium growth is observed until a critical coverage (1.5 ML) is reached. Then significant changes in the photoelectron spectra take place followed by gallium droplet formation. There is only a weak interaction of gallium atoms with the silicon substrate since a (7 × 7) diffraction pattern was observed up to relatively high coverages (1 ML).

During the annealing of the Ga layers prepared at room and low temperatures desorption of metallic gallium (observed by vanishing the metallic Ga peak) occurred. Above 360 °C only island bases with metallic gallium in the second layer were observed. The second layer atoms are characterized by a metallic-Ga peak but no Fermi edge has been observed. This indicates differences in electronic properties of the second and third gallium layers formed on the island bases.

In addition to the previously reported structures a new ($3\sqrt{3} \times 3\sqrt{3}$) R30° reconstruction was observed both during high temperature deposition and subsequent annealing of layers. The structure is stable in a narrow temperature range and forms an intermediate step between the ($\sqrt{3} \times \sqrt{3}$) R30° reconstruction and the island structure. A real-space model consisting of four gallium atom clusters corresponding to this reconstruction was also proposed; however, further experiments are needed to confirm it.

Acknowledgments

This work was supported by the research grant schemes of the Ministry of Education CR (MSM0021630508 and LC1360011). We also wish to acknowledge the help of an MSB team at the Elettra Synchrotron Light Laboratory in Trieste.

References

[1] Shibata M, Stoyanov S S and Ichikawa M 1999 *Phys. Rev.* B **59** 10289
[2] Yasuda T, Yamasaki S and Gwo S 2000 *Appl. Phys. Lett.* **77** 3917
[3] Kawazu A and Sakama H 1988 *Phys. Rev.* B **37** 2704

[4] Zegenhagen J, Hybertsen M S, Freeland P E and Patel P J 1988 *Phys. Rev.* B **38** 7885
[5] Zegenhagen J, Patel J R, Freeland P E, Chen D M, Golovchenko J A, Bedrossian P and Northrup J E 1989 *Phys. Rev.* B **39** 1298
[6] Chen D M, Golovchenko J A, Bedrossian P and Mortensen K 1988 *Phys. Rev. Lett.* **61** 2867
[7] Patel J R, Zegenhagen J, Freeland P E, Hybertsen M S, Golovchenko J A and Chen D M 1989 *J. Vac. Sci. Technol.* B **7** 894
[8] Lai M Y and Wang Y L 1999 *Phys. Rev.* B **60** 1764
[9] Lai M Y and Wang Y L 2000 *Phys. Rev.* B **61** 12608
[10] Lai M Y and Wang Y L 2001 *Phys. Rev.* B **64** 241404(R)
[11] Schmidt J, Ibach H and Müller J E 1995 *Phys. Rev.* B **51** 5233
[12] Hanada T, Daimon H, Nagano S, Ino S, Suga S and Murata Y 1997 *Phys. Rev.* B **55** 16420
[13] Jia J-F, Liu X, Wang J-Z, Li J-L, Wang X S, Xue Q-K, Li Z-Q, Zhang Z and Zhang S B 2002 *Phys. Rev.* B **66** 165412
[14] Ohtake A 2006 *Phys. Rev.* B **73** 033301
[15] Tsay S-F, Tsai M-H, Lai M Y and Wang Y L 2000 *Phys. Rev.* B **61** 2699
[16] Paggel J J, Theis W, Horn K, Jung C, Hellwig C and Petersen H 1994 *Phys. Rev.* B **50** 18686
[17] Piancastelli M N, Paggel J J, Weindel C, Hasselblatt M and Horn K 1997 *Phys. Rev.* B **56** R12727
[18] Himpsel F J, Hollinger G and Pollak R A 1980 *Phys. Rev.* B **28** 7014
[19] Demuth J E, Thompson W J, DiNardo N J and Imbihl R 1986 *Phys. Rev. Lett.* **56** 1408
[20] Landemark E, Karksson C J, Chao Y-C and Uhrberg R I G 1992 *Phys. Rev. Lett.* **69** 1588
[21] Althainz P, Myler U and Jacobi K 1991 *Phys. Rev.* B **43** 14157
[22] Fritsche R, Wisotzki E, Islam A B M O, Thissen A, Klein A, Jaegermann W, Rudolph R, Tonti D and Pettenkofer C 2002 *Appl. Phys. Lett.* **80** 1388
[23] Lüth H 1997 *Surfaces and Interfaces of Solid Materials* 3rd edn (Berlin: Springer) p 336 and 383
[24] Hamers R J, Tromp R M and Demuth J E 1986 *Phys. Rev. Lett.* **56** 1972
[25] Fritsche R, Wisotzki E, Thißen A, Islam A B M O, Klein A, Jaegermann W, Rudolph R, Tonti D and Pettenkofer C 2002 *Surf. Sci.* **515** 296
[26] Yeom H W, Abukawa T, Takakuwa Y, Fujimori S, Okane T, Ogura Y, Miura T, Sato S, Kakizaki A and Kono S 1998 *Surf. Sci.* **395** L236
[27] Cho S W, Nakamura K, Koh H, Choi W H, Whang C N and Yeom N W 2003 *Phys. Rev.* B **67** 035414
[28] Kinoshita T, Kono S and Sagawa T 1986 *Phys. Rev.* B **34** 3011
[29] Kolibal M, Prusa S, Plojhar M, Babor P, Potocek M, Tomanec O, Kostelnik P, Markin S N, Bauer P and Sikola T 2006 *Nucl. Instrum. Methods Phys. Res.* B **249** 318